Quantification of plankton-sized microplastics in a productive coastal Arctic marine ecosystem

Rist, Sinja; Vianello, Alvise; Winding, Mie Hylstofte Sichlau; Nielsen, Torkel Gissel; Almeda, Rodrigo; Torres, Rocío Rodríguez; Vollertsen, Jes

Published in:
Environmental Pollution

Link to article, DOI:
10.1016/j.envpol.2020.115248

Publication date:
2020

Document Version
Peer reviewed version

Quantification of plankton-sized microplastics in a productive coastal Arctic marine ecosystem

Sinja Rist[a,b], Alvise Vianello[c], Mie Hylstofte Sichlau Winding[d], Torkel Gissel Nielsen[a], Rodrigo Almeda[a], Rocío Rodríguez Torres[a], Jes Vollertsen[c]*

[a]National Institute of Aquatic Resource, Technical University of Denmark, Kemitorvet, Kongens Lyngby, Denmark

[b]Department of Environmental Engineering, Technical University of Denmark, Bygningstorvet, Kongens Lyngby, Denmark

[c]Department of the Built Environment, Aalborg University, Thomas Manns Vej 23, Aalborg Øst, Denmark

[d]Greenland Climate Research Centre, Greenland Institute of Natural Resources, Kivioq 2, Nuuk, Greenland

* Corresponding author: siri@env.dtu.dk

Abstract

Microplastics (MPs) are polluting the Arctic, but our understanding of their abundance, distribution, and sources is limited. This study quantified MPs down to 10 µm in marine waters of the most populated region in Greenland. A new plastic-free pump-filter system was used to collect MPs from surface waters in the fjord Nuup Kangerlua close to Nuuk. Additionally, we took samples by horizontal tows with a bongo net (300 µm mesh-size). The median concentrations were 142 MPs m^{-3} and 0.12 MPs m^{-3} in the pump and bongo samples, respectively. The most abundant polymer was polyester across stations and sampling types. Fibers were the dominant shape in the bongo samples, while non-fibrous particles dominated in the pump samples. MP abundance was lower in the fjord and increased close to Nuuk and towards the open ocean, indicating that Nuuk is an important point source for MPs. In both samples, concentrations of MPs increased with decreasing size, illustrating the importance of quantifying the smallest fraction of MPs. Thus, the use of methods allowing for a quantification of the smallest MPs is vital to reduce the underestimation of MP concentrations in the environment. The smallest size fraction is also most available to plankton-feeding marine invertebrates and an important entry point for MPs into marine food webs. At the found concentrations, immediate adverse effects on the pelagic food webs are unlikely. However, growing anthropogenic activities could increase the risk of MPs to affect the sensitive Arctic ecosystem.

Capsule:

Sampling of microplastics >10 µm in West Greenland with a new pump system demonstrated the dominance of the smallest size fraction, which is the most likely to enter pelagic marine food webs.

Keywords: Greenland; plastic pollution; pump-filter system; bongo net; µFTIR-Imaging

Introduction

It is well documented that microplastics (MPs, <5 mm) have already polluted the most remote areas on earth, such as the polar regions (Cincinelli et al., 2017; Lusher et al., 2015; Obbard et al., 2014). In the Arctic, MPs have already been detected in marine waters (Morgana et al., 2018; Tekman et al., 2020), sediments (Bergmann et al., 2017), sea ice (Peeken et al., 2018), and snow (Bergmann et al., 2019). Although data on MP concentrations in the Arctic is still very limited, a wide range of concentrations has been reported for Arctic seawater: from 0.0007 to 31,300 MPs m^{-3} (Table 1). Especially in sea ice and snow surprisingly high concentrations have been documented; for instance up to $1.2 \cdot 10^7$ MPs m^{-3} in ice cores of Fram Strait (Peeken et al., 2018). The total load of plastics floating on the surface of the Arctic Ocean has been estimated to range between 100 and 1200 tons (Cózar et al., 2017), and global modeling of the distribution and accumulation of marine debris identified a garbage patch in the Barents Sea (van Sebille et al., 2012). These high levels of plastic pollution in an area with extremely low direct anthropogenic impact can to a great extend be explained by long-range transport of plastics with air and currents (Obbard, 2018). Atmospheric deposition has only recently been identified as a major pathway for global MP transport (Brahney et al., 2020) and can most likely explain high concentrations of MPs in Arctic snow samples (Bergmann et al., 2019). In contrast, long-distance transport by currents is well known and the poleward branch of the Thermohaline Circulation is a major pathway of plastics from the North Atlantic to the Greenland and Barents Sea (Cózar et al., 2017). Model simulations suggest that these areas are accumulation zones for plastics, holding 95% of the estimated plastic load in the Arctic. This was corroborated by field measurements (Cózar et al., 2017). One branch of the Thermohaline Circulation also goes into the Labrador Sea, but except for the study by Cózar et al. (2017), no data on MP pollution is available from the west coast of Greenland.

West Greenland receives plastic debris from the North Atlantic as well as from local point sources. Relevant point sources of plastic pollution include fishing and maritime industry, raw sewage outlets, mismanaged waste, and last but not least Nuuk, the capital and largest city of Greenland with 18,000 inhabitants. Nuuk holds the biggest port of Greenland and the city's wastewater is discharged untreated to the fjord Nuup Kangerlua (Gunnarsdóttir et al., 2013). Thus, there are several unquantified sources of MP pollution in West Greenland. If MPs introduced to the marine ecosystem are taken up by the marine food web, Greenlandic livelihood may be impacted. Fishery alone provides more than half of Greenland's export income (Jacobsen et al., 2018). If the food web efficiency or the quality of the marine products are affected by MPs, it will potentially have a major impact on the local and national economy of Greenland.

The present study is the first to focus on marine MPs in the most populated area of Greenland. Furthermore, we applied a new plastic-free pump-filter system, which allows the collection and full quantification of MPs down to 10 µm. Very few studies have quantified MPs down to that size in the Arctic (Table 1). This abundant and understudied fraction of MPs overlaps in size with the planktonic prey of the dominant secondary producers in the Arctic, the *Calanus* copepods (Cole et al., 2013; Levinsen and Nielsen, 2002). The large lipid-rich *Calanus* copepods have a key position in the Arctic marine ecosystem. They provide food for the important Greenlandic fish stock and are responsible for carbon sequestering through the export of carbon to the deep waters and sediment by the production of large, fast-sinking fecal pellets (Juul-Pedersen et al., 2006). The presence of plankton-sized marine MPs in the highly productive coastal ecosystem around Nuuk gives rise to concern for the quality of the important commercial and recreationally exploited fish stocks (Jacobsen et al., 2018). Therefore, the present study aims to provide a baseline of plankton-sized MPs (>10 µm) from the fjords of Greenland and the coastal area towards the potentially most important point source of MPs in West Greenland: the capital Nuuk.

Materials and Methods

Study site

The sampling of six stations in Nuup Kangerlua, in the bay in front of Nuuk, and at the banks off the coast of West Greenland, was done from the research vessel R/V Sanna (Greenland Institute of Natural Resources) between 10 and 12 of May 2019. The stations differed in their proximity to the expected MP point source Nuuk (Fig. 1, see more details in SI). Nuup Kangerlua is located on the southwest coast of Greenland with the capital Nuuk (64°10′N, 51°44′W) located at the mouth of the fjord. The average depth is approximately 250 m (max. depth >600 m) (Mortensen et al., 2011). The main fjord branch is approximately 190 km long, and several sills characterize the outer part of the fjord. The uppermost branch of Nuup Kangerlua connects the marine environment to the margin of the Greenland Ice Sheet. The freshwater input induces a seasonal stratification of the upper part of the water column (Fig. 1), which is further strengthened by solar heating during summer (Mortensen et al., 2013, 2011).

CTD measurements

On arrival at the sampling station, vertical profiles of water temperature, salinity, density, and fluorescence were obtained using a CTD (SBE 19plus V2 CTD from Sea-Bird Electronics) equipped with a Seapoint chlorophyll *a* fluorometer and a Biospherical/Licor sensor. Depth profiles were recorded from the surface to 5 m above the bottom. Water samples for chlorophyll *a* (chl *a*) measurements were collected at 1, 5, 10, 15, 20, 30, 40, 50, 100, 150, 250, and 300 m depth using a 5 L Niskin bottle between 1 and 2 of May. Each sample was filtered onto a GF/F filter and extracted in 96% ethanol for 12–24 h (Jespersen and Christoffersen, 1987). Fluorescence was measured on a Turner TD-700 fluorometer (Turner Designs, California, USA) before and after acidification. The

fluorometer was calibrated against a pure chl *a* standard. The analysis was used for calibration of the CTD fluorometer, and chl *a* concentrations were then calculated from CTD fluorescence profiles at all stations. The phytoplankton biomass was calculated from the average chl *a* in the upper 10 m, a carbon/chl *a* conversion factor of 42.6 (Juul-Pedersen et al., 2006) and a carbon to dry weight conversion factor of 55% (Hansen et al., 1994).

MP sampling

Two different sampling devices were employed to collect one sample each at the six stations. We collected MPs >10 µm from 5 m depth using a custom made pump-fed filtering device (hereinafter termed "pump samples"). In addition, we took surface samples with a submerged bongo net targeting >300 µm sized MPs (hereinafter termed "bongo samples"). The plastic-free pump-filter system was developed to sample the smallest fraction of MPs, which is often neglected in other studies. The purpose of the bongo samples was to allow comparability to previous studies using this and similar net-sampling techniques. Both samples were taken in the upper 5 m, i.e., above the pycnocline (Fig. 1), in the water impacted by the meltwater from the inner part of the fjord system. Unfortunately, the bongo sample from station 1 was lost during transportation, resulting in only 5 stations for this sampling method.

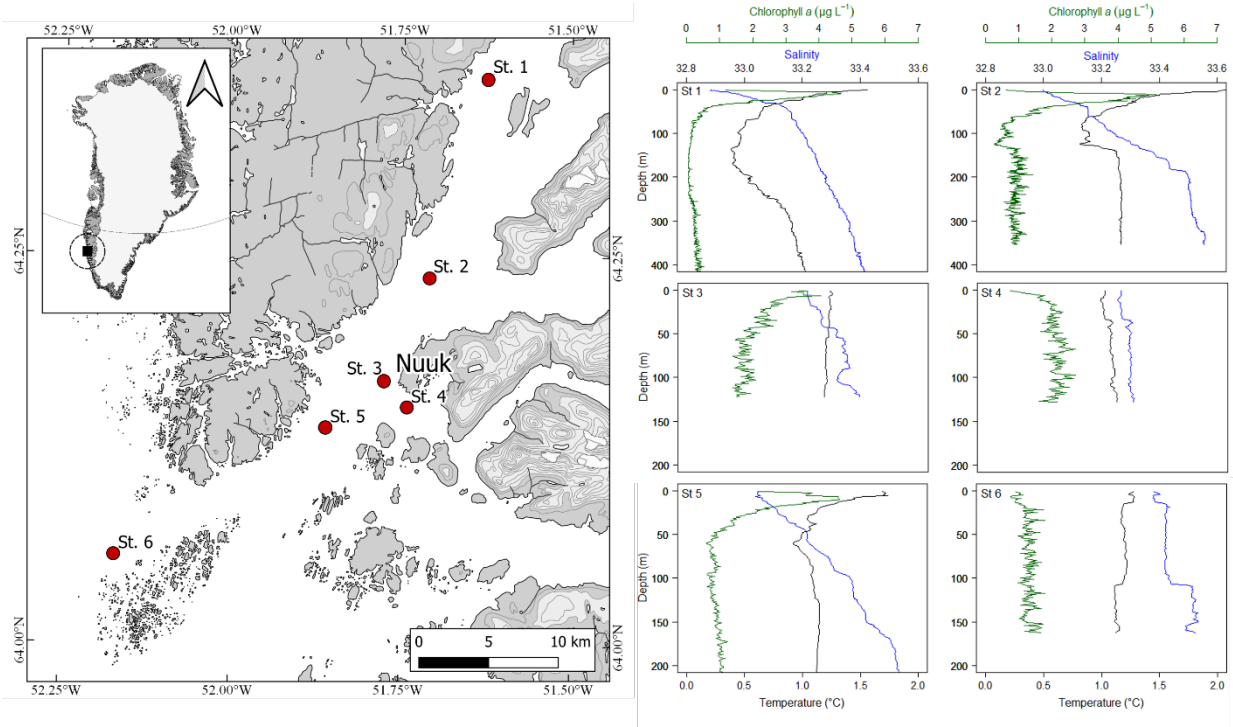

Figure 1. Sampling stations in Nuup Kangerlua with respective CTD and chlorophyll *a* profiles.

The plastic-free pump-filter device (UFO system - Universal Filtering Objects system) was composed of a metal hose deployed in the water, a pump controlled by an inverter, and a modular filtering device capable of filtering large volumes of water (Fig. S1, SI). All parts of the system were in metal but for a gasket of rubber in the three filtering cartridges themselves. In brief, the water was pumped through a flexible metal hose, the mouth of which was equipped with a stainless steel metal cage of 5 mm mesh to protect the system against large debris. A positive displacement pump with a brass impeller (Oberdorfer Gearpump N994RE) sent the water through a short metal hose to the filter cartridges. Three separate stainless steel filter cartridges were applied, which each contained a stainless steel filter of 167 mm diameter. The water first passed through a filter of 300 µm mesh to retain bigger items with the purpose of protecting the finer filtering mesh from clogging. The water was then divided onto two parallel units with filters of 10 µm. The outlets were

136 re-combined and connected to a mechanical flowmeter to quantify the filtered volume. The inlet
137 hose was deployed at 5 m depth using a crane, and approximately 1 m^3 of water was filtered at each
138 station. After sampling, the system was evacuated, and the single filter cartridges were opened
139 inside a clean fume hood to prevent plastic contamination. Both the 300 µm and the two 10 µm
140 enriched filters collected at each station were transferred to a glass petri dish, which subsequently
141 was wrapped in aluminum foil and frozen at -20°C until sample processing. Three air blanks were
142 taken during the sampling by exposing empty petri dishes with pre-muffled 10 µm steel filters to
143 the surrounding environment during the opening phase of the UFO system. The air-blanks were
144 taken and stored similarly to the samples. Moreover, several paint fragments were collected
145 onboard the ship to assess the potential contamination related to this specific source.

146 The bongo net, equipped with a flowmeter, was deployed 3 m from the side of the ship using a
147 crane and dragged for 20 min in the upper 0.5 m of the water column. The net was made of nylon, it
148 had a mesh size of 300 µm, and the samples were collected in the cod-end of the net. The bottle at
149 the cod-end was removed from the net, and the content was carefully rinsed onto a 300 µm nylon
150 mesh. The mesh was carefully folded, wrapped in aluminum foil, and stored in a polyethylene
151 plastic zip-lock bag at -80°C until sample processing.

152 **Sample processing**

153 The pump samples were processed following a protocol slightly modified from Liu et al. (2019)
154 (see SI for details). In brief, this included six treatment steps: 1) SDS (5% sodium dodecyl sulfate)
155 treatment for 24 h and transfer of samples onto 10 µm steel filters (47 mm diameter), 2) overnight
156 incubation with protease (Sigma, Protease from *Bacillus sp.*) and lipase (Strem Chemicals,
157 Lipozyme® TL 100L), 3) incubation with cellulase (Sigma, Cellulase enzyme blend) and
158 Viscozyme® L (Sigma) for 72 h, 4) oxidation (Fenton reaction) with hydrogen peroxide, sodium

hydroxide and iron sulfate overnight, 5) size fractionation with a 500 µm steel sieve, 6) density separation of the fraction <500 µm with sodium polytungstate (1.9 g cm^{-3}). The fraction >500 µm underwent spectroscopic analysis together with the bongo samples. The filter with the sample fraction <500 µm was sonicated and rinsed with 50% ethanol, and all liquid was sequentially transferred to 10 mL glass vials and evaporated in a water bath at 50°C using a stream of nitrogen (Biotage, TurboVap). When the samples were dry, 5 mL of 50% ethanol were added for subsequent analysis with FPA-µFTIR-Imaging (Focal Plane Array-Fourier-Transform Infrared Imaging-micro Spectroscopy). The collected air-blanks from the ship underwent the same processing and analysis in the laboratory as the pump samples. Thus, the blank samples monitor the combined MP contamination potentially occurring onboard and later during sample processing and analysis.

For the bongo samples we used a simplified protocol. The samples were rinsed off the mesh into glass beakers with a 5% SDS solution and kept at 50°C with gentle stirring (100 rpm) for 48 h. The samples were then sieved over a 200 µm stainless steel sieve, rinsed with filtered water, and flushed back into the beaker with 200 mL of Tris (trisaminomethane)-HCl buffer (pH 8.3), adding 700 µL of protease, 500 µL of lipase, and incubating at 50°C with gentle stirring for 72 h. Thereafter, samples were vacuum-filtered onto 10 µm stainless steel filters (47 mm diameter) and stored in glass petri dishes until analysis.

MP analysis

The pump samples were analyzed using FPA-µFTIR-Imaging, which is, at present, considered the most suitable analytical approach for analysis of small MPs (Liu et al., 2019; Löder et al., 2015; Mintenig et al., 2016; Primpke et al., 2016; Simon et al., 2018; Vianello et al., 2019). A sub-sample of the 5 mL particle suspension (3 aliquots of 1-1.2 mL – corresponding to 60-72% of the total volume) was deposited onto three 13×2 mm zinc selenide (ZnSe) infrared windows pre-heated and

held in a compression cell (PIKE Technologies, Fitchburg, WI, USA) using a capillary glass pipette (micro-classic, Brand GmbH, Germany). Each enriched window was dried overnight (55°C) and subsequently analyzed, accounting for the whole active surface (10 mm diameter - 78.5 mm^2). The applied instrument was an Agilent 620 FTIR microscope with a 128×128-pixel FPA detector combined with a Cary 670 FTIR spectrometer (Agilent Technologies, Santa Clara, CA, USA). It provides two main outputs: a magnified optical image, and the relative IR map of stitched tiles of 128×128 pixels, co-adding several scans. Each IR map pixel contains an FTIR spectrum, allowing the identification of a wide range of organic and inorganic materials (including synthetic polymers) by comparing the unknown spectra with a dedicated database. The analysis was carried out in transmission mode in a spectral range of 3750-850 cm^{-1} at 8 cm^{-1} resolution, using a 15x Cassegrain objective/condenser with 5.5 µm resulting pixel size; 120 co-added scans were collected for the background on a single tile, while 30 co-added scans were recorded when scanning the sample. The beam attenuation was 50%. The scan time at these settings was approximately four hours.

The bongo samples were visually inspected using a stereo microscope with a connected camera (SteREO Discovery V8 with Axiocam 105 Color, Zeiss GmbH, Oberkochen, Germany). All potential plastic particles were photographed and categorized by shape (fibers vs. all other shapes), length, and width. The material composition of each particle was then analyzed by Attenuated Total Reflection – Fourier Transform Infrared Spectroscopy (ATR-FTIR), using an Agilent Cary 630 FTIR spectroscope (Agilent Technologies, Santa Clara, CA, USA) with a single reflection diamond ATR. The samples were positioned onto the ATR crystal and then compressed using the instrument clamp to achieve optical contact, allowing to record surficial ATR-FTIR spectra. The spectra were recorded at 4 cm^{-1} spectral resolution by co-adding 64 scans, and a background in air was collected before each measurement. Each collected spectrum was exported and compared to multiple spectral

databases containing both synthetic polymers and non-synthetic materials (Omnic 8, Thermo Fisher Scientific, Madison, WI, USA).

Contamination control

The use of plastic materials during sampling and sample processing was avoided if possible, except for the polytetrafluoroethylene (PTFE) stopcock of the separation funnels and the PTFE septa of the vials containing the processed pump samples. Therefore, this material, together with the rubber from the UFO gaskets, was excluded from the MP quantification. Furthermore, we took samples of the ship's paint and excluded matching paint particles in the samples. For the bongo samples, potential contamination could have resulted from the nylon mesh as well as the polyethylene zip-lock bags. All materials were either rinsed with filtered water or muffled at 500°C and wrapped in aluminum foil until use. Samples were also covered with aluminum foil or glass lids whenever possible. All solutions used for processing the samples were filtered over 0.7 or 1.2 µm GF filters. Sample processing was done in a laminar flow cabinet, and cotton lab coats were worn. As described above, three air-blank samples were collected on the ship during sampling, which underwent the same laboratory processing and analysis as the real samples. They therefore represent the total contamination, from sampling until sample analysis.

Data analysis

The collected FPA-Imaging data were processed using siMPle (Primpke et al., 2020), an open-source software developed by Aalborg University and Alfred Wegener Institute, which allows the automated analysis of large µFTIR-Imaging datasets. In brief, it runs a Pearson correlation between each sample spectrum and the database using the raw spectrum, first and second derivative, reconstructing each particle from the FTIR spectra of the pixels it covers, and hence providing a false-color map of the identified materials in the sample. The software also provides morphological

and size measurements (Vianello et al., 2019), as well as estimated mass measurements (Liu et al., 2019). With regards to particle shape, we differentiate between fibers and particles (i.e. all other shapes) as described in Vianello et al. (2019) (Fig. S3, SI). The mass of the plastic particles in the pump samples was estimated following an approach described by Simon et al. (2018). In short, the 2-dimensional size and shape of a MP particle obtained by the siMPle analysis are used to estimate a particle volume. The mass is then derived by multiplying with the typical density of the determined polymer.

Results and Discussion

MP abundance and size distribution

We found MPs in the water samples from all stations. In the pump samples (>10 µm), we found MP concentrations of 67-278 particles m^{-3}, with a median of 142 particles m^{-3} (Fig. 2a). The MP concentrations (>300 µm) found in the bongo samples were 2-3 orders of magnitude lower than those collected by the pump, ranging between 0.08 and 0.4 MPs m^{-3} with a median concentration of 0.12 MPs m^{-3} (Fig. 2b). Data on MPs in Arctic waters is scarce, and a wide range of concentrations has been reported (Table 1). The results of the bongo samples are in a similar range as what was collected using a Manta net around Svalbard (Lusher et al., 2015) and in the Chukchi and Bering Sea (Mu et al., 2019) as well as from pump samples in the Arctic Central Basin (Kanhai et al., 2018). The MP concentrations from our pump samples are comparable to recently reported values from surface water samples in the Fram Strait, where 113-262 particles m^{-3} were found (except for one station with 1287 particles m^{-3}) (Tekman et al., 2020). Tekman et al. (2020) fully quantified MPs down to 32 µm (the size of the sieve during sampling) and semi-quantified MPs down to 11 µm.

Despite the comparative remoteness of the studied area, the concentrations of MPs found in this study were similar to those reported in locations with higher anthropogenic activity. In Manta trawls close to the Danish coast, the average MP concentration was 0.07 m^{-3} (>300 µm) (Tamminga et al., 2018), and in marine waters around Japan, Isobe et al. (2015) found a median concentration of 0.74 MPs m^{-3} (>350 µm). A quantification of MPs down to 10 µm in a transect from the European coast across the Atlantic to the Sargasso Sea gave 13 to 501 MPs m^{-3}, with the highest concentrations in the English Channel (Enders et al., 2015).

Table 1. Reported MP concentrations in seawater, sea ice and snow samples in the Arctic region.

Location	Matrix and depth	MP conc. (MPs m^{-3})	Size limit (µm)	Sampling method	Dominant polymer	Reference
Nuup Kangerlua, West Greenland	Water, 5 m Water, surface	142 0.12	10 300	Pump Bongo net	Polyester	This study
Greenland Sea Gyre	Water, surface	800-3740	50	Pump and plankton net	Polyester	[1]
East Greenland	Water, 0-50 m	2.38 (2014)	500	WP-2 net	Polyester	[2]
Northeast Greenland	Water, 6 m	2.4	80	Water intake	Polyethylene	[3]
Greenland & Barents Sea	Water, surface	$6.3 \cdot 10^4$ km^{-2}	500	Manta trawl	-	[4]
Fram Strait	Water, 1-5350 m	95	32	McLane WTS-LV	Polyamide	[5]
Fram Strait, Svalbard	Snow	$1.76 \cdot 10^6$	11	Sampled with a spoon	Acrylates/PUR/varnish	[6]
Svalbard	Water, surface Water, 6 m	0.34 2.68	333 250	Manta trawl Onboard pump	Polyester, polyamide	[7]
Svalbard*	Water, 0-1000 m Sea ice, free float	0.0007-0.048 0.158	50	Niskin bottles Boat hook	Paint Unknown pigment	[8]
Arctic central basin	Water, 8.5 m Water, 8-4369 m	0.7 20.8	250	Water intake Niskin bottles	Polyester	[9]
Arctic	Water, surface	31,300	100	1 L grab samples	Polyester	[10]
Central Arctic	Sea ice	$0.38\text{-}2.34 \cdot 10^5$	0.22	Drilling of ice cores	Rayon	[11]
Arctic	Sea ice	$0.11\text{-}1.2 \cdot 10^7$	11	Drilling of ice cores	Polyethylene	[12]
Arctic Central Basin	Sea ice	$0.2\text{-}1.7 \cdot 10^4$	100	Drilling of ice cores	Polyester	[13]

	Water below ice	0-18	250	Pump and sieve		
Chukchi Sea	Water, surface	0.23	330	Manta trawl	Polyethylene terephthalate	[14]
Bering Sea		0.091				

*Quantified all anthropogenic particles, including non-synthetic. [1] (Jiang et al., 2020), [2] (Amélineau et al., 2016), [3] (Morgana et al., 2018), [4] (Cózar et al., 2017), [5] (Tekman et al., 2020), [6] (Bergmann et al., 2019), [7] (Lusher et al., 2015), [8] (von Friesen et al., 2020), [9] (Kanhai et al., 2018), [10] (Barrows et al., 2018), [11] (Obbard et al., 2014), [12] (Peeken et al., 2018), [13] (Kanhai et al., 2020), [14] (Mu et al., 2019)

Other studies from the Arctic report both lower and higher MP concentrations in comparison to our findings (Table 1). Several factors, however, complicate comparisons between studies. Firstly, the Arctic covers a vast area and the sampled locations differ greatly with regards to oceanographic regimes and potential MP sources. Since our study is the first to analyze MPs on the west coast of Greenland, the closest available data on MPs comes from East Greenland. There, long-range transport is expected to play a much bigger role, while local sources are more relevant for West Greenland (see MP distribution and sources). Secondly, studies employed widely different methodologies for sampling, sample preparation, and analysis, as well as the analyzed size fractions. The problems with lack of standardization are frequently emphasized within the MP field (e.g., Avio et al., 2017; Mai et al., 2018). The impact of the chosen methodology on the results becomes very apparent when comparing our two sampling methods. The concentrations from the pump and the bongo net differed by 2-3 orders of magnitude. This is likely related to several factors. While the particle identification and quantification of the pump samples were fully automated, the analysis of the bongo samples relied on visual pre-sorting, which entails the risk of missing particles. More importantly though, the lower size limit was very different, with 10 µm for the pump and 300 µm for the bongo net. The results of our pump samples clearly show an increase in particle numbers with decreasing size (Fig. 2e). The size distribution was similar for all stations (Fig. S2, SI). Overall, 93% of all the particles we found were smaller than 300 µm and 68% smaller than 100 µm. Only for the size fraction of 11-25 µm we found very few particles. This is most likely related to the detection limit of the µFTIR approach, which is limited to around 11 µm due to

281 diffraction phenomena. The spectra of very small and thin particles often have a low signal-to-noise
282 ratio, affecting their automatic identification by the siMPle software, probably leading to an
283 underestimation of the smallest MP particles. The size distribution in the bongo samples showed a
284 similar trend of higher particle numbers with decreasing size, with the exception of a large number
285 of very big particles (>5000 µm) (Fig. 2f). These were mainly long fibers, which were also the
286 dominant particle shape in the bongo samples (see MP shape and polymer composition). Similar
287 size distributions as in our pump samples were found in studies on Arctic sea ice (Peeken et al.,
288 2018), snow (Bergmann et al., 2019), and water samples (Tekman et al., 2020), which also analyzed
289 MPs down to 11 µm. This finding clearly illustrates the importance of quantifying the smallest
290 MPs. Since the majority of published studies on MP concentrations in marine waters used a mesh
291 size that is considerably larger, concentrations are generally underestimated at present. Therefore,
292 we encourage the use of pump-filter systems as used in the present study or similar devices, which
293 enable sampling the smallest size fraction of MPs that can be analyzed.

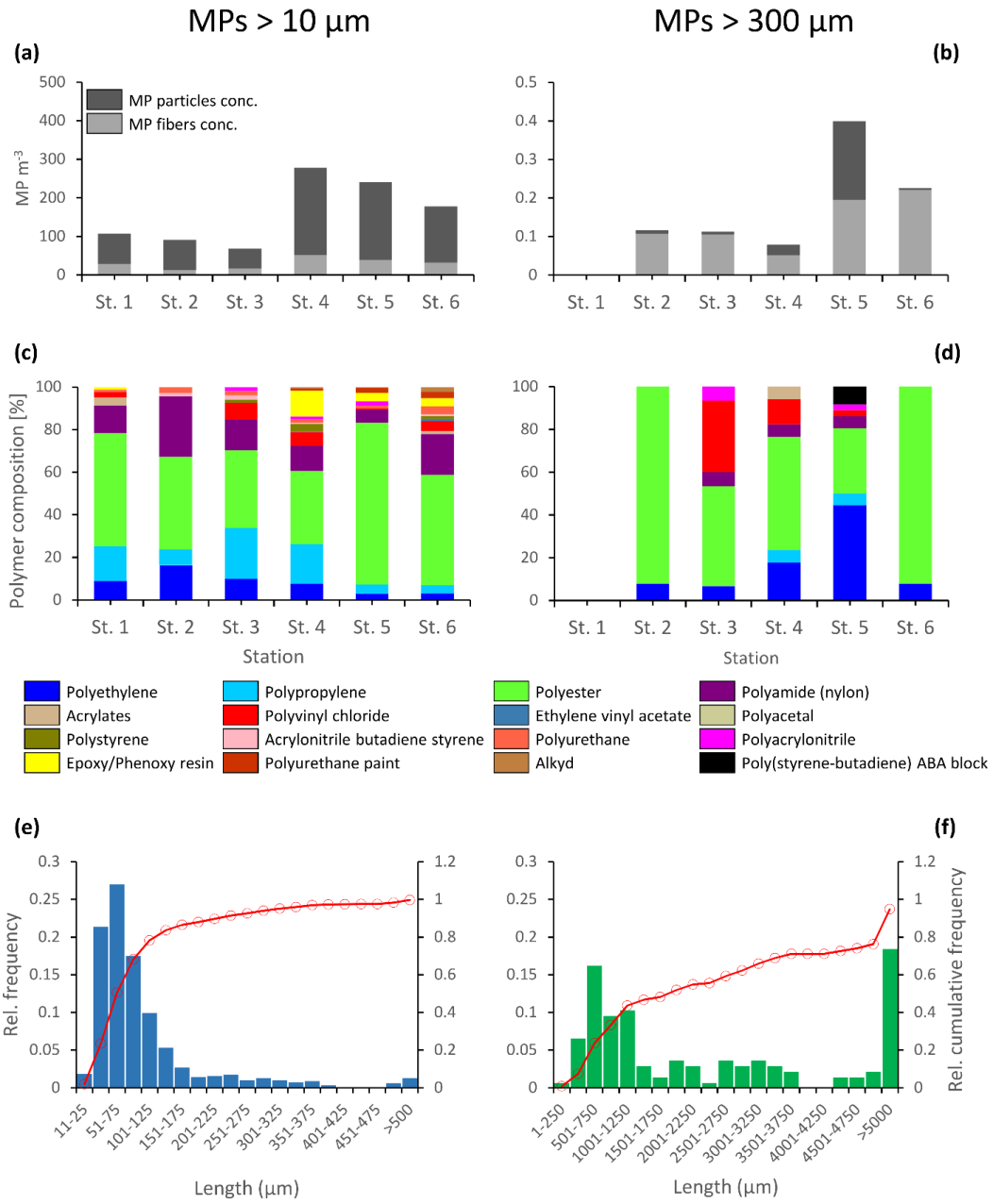

294

295 **Figure 2.** Microplastics (MPs) from pump (left panels) and bongo (right panels) samples: MP
296 concentration (MPs m^{-3}) in (a) the pump and (b) the bongo samples; Polymer composition (%) in
297 (c) the pump and (d) the bongo samples; Size distribution (length - µm) in (e) the pump and (f) the
298 bongo samples. The red line in (e) and (f) shows the relative cumulative frequency of MPs.

299

300 **Blank samples**

301 The blank samples contained both the on-site airborne contamination and the contribution derived
302 from the laboratory. The results showed an average contamination of 6.7 ± 2.5 MPs per sample,
303 corresponding to 4.8 ± 2.5% of the average MP abundance in the analyzed samples. The polymeric
304 composition of the contaminating MPs was 50% polyester, 25% polyamide (nylon), 17% ethylene
305 vinyl acetate, and 8% polystyrene. The results were corrected for contamination by subtracting the
306 averaged contribution of every single polymer found in the blank samples (both by particle number
307 and mass). The polyester and nylon items identified in the blank samples could be related to
308 airborne contamination from textiles, as most of the technical clothes used onboard are made of
309 these polymers. The ship paints were another relevant source of contamination found in the
310 analyzed samples, but not in the blanks. Several paint particles were identified by µFTIR-Imaging
311 analysis as the specific paints collected onboard from different surfaces of the ship during the
312 survey. This specific contribution was excluded from the results. However, this finding stresses the
313 importance of monitoring every source of potential contamination to reduce bias in MP analysis.

314 **MP shape and polymer composition**

315 Fibers were found in all samples, but while they comprised the minority of shapes in the pump
316 samples (18%), fibers were the dominant shape in the bongo samples (73%) (Fig. 2a, b). Fibers
317 were also the predominant shape in Manta trawls (333 µm mesh) close to Svalbard (Lusher et al.,
318 2015) and vertical tows with a plankton net (500 µm mesh) in East Greenland (Amélineau et al.,
319 2016). The most common polymer from both sample types was polyester, except for the bongo
320 sample at station 5 (Fig. 2c, d). This is in accordance with other Arctic studies, which found
321 polyester to dominate (Amélineau et al., 2016; Barrows et al., 2018; Kanhai et al., 2020, 2018;

322 Obbard et al., 2014) (Table 1). One likely source for polyester is synthetic textiles, which fits with
323 the finding of fibers. It has been shown that textiles can release thousands of fibers during washing,
324 which subsequently end up in the wastewater (Napper and Thompson, 2016; Pirc et al., 2016).
325 Since Nuuk has no wastewater treatment, all fibers from washing effluent are released directly to
326 the fjord and are a highly likely source for polyester in our samples. Furthermore, polyethylene
327 terephthalate, which is part of the polyester family, is one of the most produced and used plastics,
328 e.g., for plastic bottles and packaging material. The next most common polymers were
329 polyamide/nylon, which is used for fishing nets, polyethylene and polypropylene, which are among
330 the top 5 high-production volume plastics globally, and epoxy/phenoxy resins, which are for
331 instance applied as adhesives or coatings in boats (Andrady, 2011; Hoge and Leach, 2016;
332 PlasticsEurope, 2019). Overall, the polymer composition reflects important local use of plastics:
333 fleece clothing for low temperatures, plastic packaging, fishing, and boating.

334 **MP distribution and sources**

335 The relative abundance of MPs between stations was similar for both methods applied (except for
336 station 4), illustrating that both methods give a representative description of the MP distribution. In
337 general, the distribution pattern followed the oceanography of the fjord, with the lowest MP
338 concentrations (68-107 MPs m^{-3}) at the meltwater-impacted stations inside the fjord (stations 1, 2
339 and 3) while the MP concentration peaked after passing the major point source of the capital Nuuk
340 (Fig. 2a, b). This indicates that Nuuk is an important source for MPs in this area, as illustrated by
341 the increase in MPs along the cruise track from the inner fjord and passing Nuuk towards the sea.
342 Furthermore, data on wind direction and water flow within the fjord during the sampling indicated
343 that the upper water layer was pushed out of the fjord (data not shown). This means that plastics
344 originating from Nuuk were even more likely to be found towards the outer part of the fjord. The
345 importance of local mismanagement of plastic waste in West Greenland was also confirmed by

346 beach litter monitoring, which reported the majority of plastic debris to originate from local sources
347 (PAME, 2019). This underlines the importance of local anthropogenic activities for plastic pollution
348 in comparison to long-range transport with currents, which is expected to be more prominent for
349 Greenland's east coast (PAME, 2019). Airborne transport of MPs has been suggested as an
350 important pathway. A recent study found extremely high concentrations of up to $14.4 \cdot 10^6$ MPs m^{-3}
351 in Arctic snow samples (Bergmann et al., 2019). This is a relevant finding with respect to the
352 present study as the Nuup Kangerlua is fed by meltwater runoff from the Greenland Ice Sheet,
353 terrestrial runoff, meltwater from sea ice, and calved glacial ice (Mortensen et al., 2013). A
354 considerable fraction of the water in the upper layers of Nuup Kangerlua is meltwater. Part of this is
355 old ice from the bottom of the glacier that is expected to be MP-free, but melted snow significantly
356 contributes to freshwater input into the fjord. With a MP contamination of snow as reported from
357 the Fram Strait, we would expect much higher concentrations in the surface waters of Nuup
358 Kangerlua, especially in the inner fjord. Our findings indicate that the MP contamination of snow in
359 West Greenland is most likely several orders of magnitude lower than reported by Bergmann et al.
360 (2019) and the main source of MPs in the fjord is of local origin rather than airborne. However, it is
361 important to note, once MPs enter the water column, they are also vertically exported to the
362 seafloor/deep waters by physical and biological processes (Choy et al., 2019; Long et al., 2015;
363 Möhlenkamp et al., 2018; Peng et al., 2018; Porter et al., 2018). In fact, marine sediments in the
364 deep sea are a major sink for plastic pollution (Woodall et al., 2014). More research is needed to
365 understand the distribution and fate of MPs in the Arctic ecosystem.

366 **MP mass versus number**

367 For the pump samples, mass concentrations of MPs were determined, which ranged from 9.3 to
368 51.3 µg m^{-3}, with a median of 28.8 µg m^{-3} (Fig. 3a). The polymer composition in terms of mass
369 differed from the particle number-based composition (Fig. 2c). Polyethylene constituted the highest

mass in the stations inside the fjord (stations 1 and 2), polyvinyl chloride dominated at station 3, polyester at stations 4 and 5 close to Nuuk, and polyamide was the polymer with the highest mass at station 6, close to the open ocean (Fig. 3b). Also, the distribution of MPs between stations gave a somewhat different picture than the number-based results. While the stations from Nuuk towards the open ocean (stations 4-6) still had higher concentrations than the more inward stations 2 and 3, station 1, furthest inside the fjord, showed the second-highest MP abundance (Fig. 3a). This speaks for the presence of a few larger (or heavier) plastic particles at that station. Plastic concentrations are rarely reported in terms of mass for water samples, especially for small-sized MPs, even though models of plastic input and abundance in the oceans on a big scale often report mass (Cózar et al., 2017; Jambeck et al., 2015; van Sebille et al., 2015). Cózar et al. (2017) estimated the total load of plastics floating on the surface of the Arctic Ocean to range between 100 and 1200 tons. The Arctic Ocean has an area of $1.4 \cdot 10^7$ km^2. Assuming that the surface area equals the upper 1 m of the water column, the reported mass equals a mass concentration of 7-86 $\mu g\ m^{-3}$. Although this is a rough estimate, our values fall within this range.

Our results illustrate that the decision of whether to report MPs in terms of mass or number will influence the picture that we get of the MP contamination. Both have their strengths and weaknesses. Mass concentrations on the one hand can be more informative about the sources and input of plastics into the environment. On the other hand, number-based concentrations are important in a biological context when considering organisms that interact with individual particles. In the best case, both should be reported. However, if only one is chosen, this choice should be based on a thorough consideration of what the results will be used for.

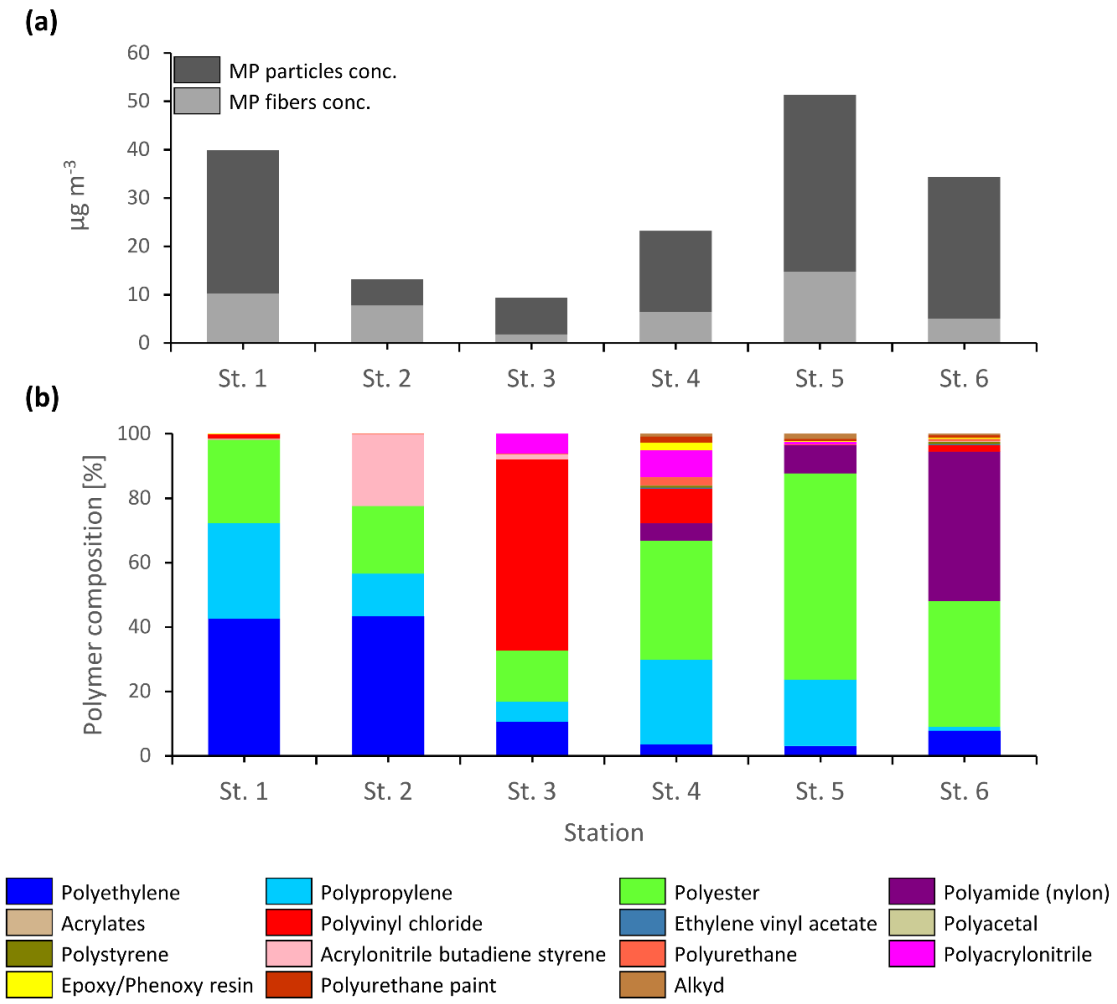

Figure 3. (a) Mass-based microplastic (MP) concentrations (µg m^{-3}) of the pump samples and (b) polymer composition based on estimated mass.

Biological implications

The dominant size fraction of MPs found in the fjord is the most available for plankton-feeding marine invertebrates. These particles overlap in size with their natural prey, and the ingestion of MPs between 7 and 150 µm has, for instance, been observed for different copepod species (Cole et

al., 2013; Sun et al., 2017; Vroom et al., 2017). The high abundance and vital role of copepods in the Arctic ecosystem illustrate their key position as an entry point for MPs into Arctic food webs. However, compared to their phytoplankton prey, the mass of plankton-sized MPs is more than 3-4 orders of magnitude lower than that of phytoplankton (Fig. 4), which illustrates the low probability for ingestion and impact on zooplankton. The ratio between phytoplankton and MPs depends, however, on the location. While the ratio was high in the inner fjord due to a phytoplankton bloom, it was considerably lower from Nuuk towards the open ocean (stations 4-6) (Fig. 4). This means that the likelihood for a plankton-feeding organism to ingest MPs differs greatly between stations, depending on the phytoplankton biomass "background". Benthic invertebrates like crustaceans and bivalves, as well as fish, have been found to contain MPs (Abbasi et al., 2018; Davidson and Dudas, 2016; Devriese et al., 2015; Li et al., 2018). Furthermore, studies have documented the trophic transfer of MPs (Setälä et al., 2014; Welden et al., 2018). Thus, MP pollution is of concern to marine food webs. However, at the concentrations of MPs found in this study, a minor impact on the Arctic pelagic food web is expected. Still, in a predicted scenario of increasing plastic pollution (Lebreton et al., 2019; Lebreton and Andrady, 2019) and accelerated melting of Arctic sea ice, increased MP pollution, together with other anthropogenic stressors, could negatively affect the Arctic pelagic food web. This could be a major concern for the fishing and seafood sector in Greenland in the future, where the economy heavily depends on unpolluted marine resources (Jacobsen et al., 2018). Therefore, it is of paramount importance to get a better understanding of the sources, distribution, and abundance of MPs in the Arctic waters, and to reduce global plastic pollution that will end up in the Arctic.

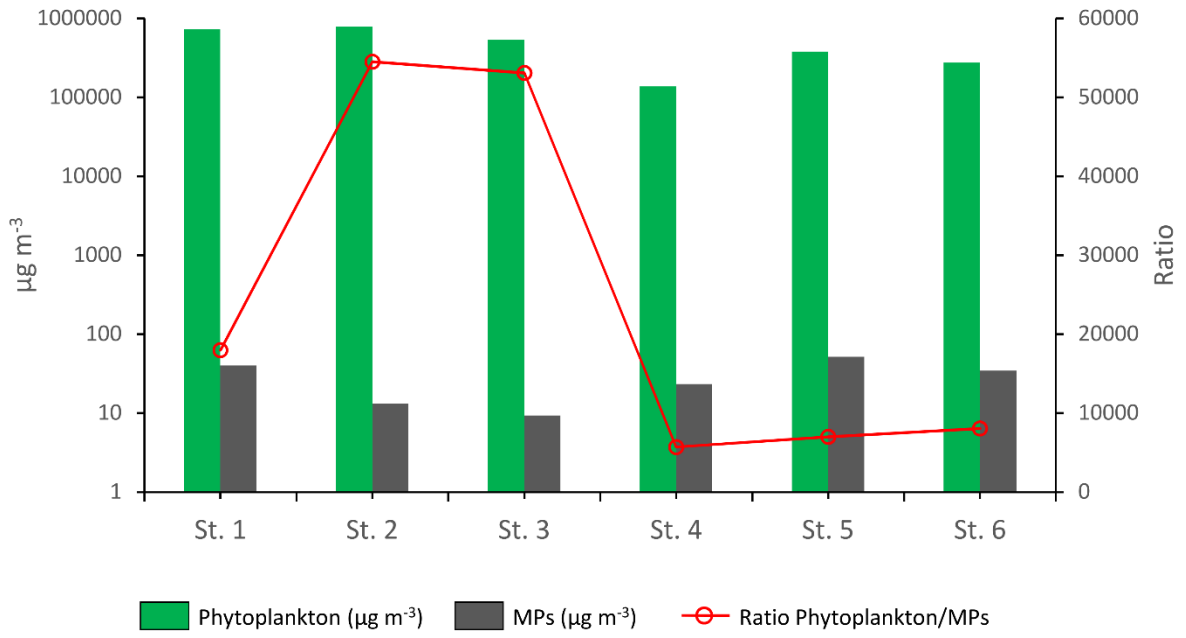

420

421 **Figure 4.** Mass concentrations (µg m^{-3}) of phytoplankton (green), based on the fluorescence
422 measurements of the CTD, and microplastics (MPs) (grey) at the six sampling stations. The red line
423 shows the ratio of phytoplankton to MPs in terms of mass.

Acknowledgements

We thank the crew on R/V Sanna for their help during the sampling. For financial support, we would like to thank the Velux foundation through the project MarinePlastic (Project no. 25084). This paper was furthermore supported by the H2020 CLAIM project (Cleaning Litter by developing and Applying Innovative Methods in European seas; Grant Agreement No. 774586) to TGN and a research grant ("Microplastic" project no. 39610, 2019) from the Maritime DTU-Orients Fund to RA.

References

Abbasi, S., Soltani, N., Keshavarzi, B., Moore, F., Turner, A., Hassanaghaei, M., 2018. Microplastics in different tissues of fish and prawn from the Musa Estuary, Persian Gulf. Chemosphere 205, 80–87. https://doi.org/10.1016/j.chemosphere.2018.04.076

Amélineau, F., Bonnet, D., Heitz, O., Mortreux, V., Harding, A.M.A., Karnovsky, N., Walkusz, W., Fort, J., Grémillet, D., 2016. Microplastic pollution in the Greenland Sea: Background levels and selective contamination of planktivorous diving seabirds. Environ. Pollut. 219, 1131–1139. https://doi.org/10.1016/j.envpol.2016.09.017

Andrady, A.L., 2011. Microplastics in the marine environment. Mar. Pollut. Bull. 62, 1596–1605. https://doi.org/10.1016/j.marpolbul.2011.05.030

Avio, C.G., Gorbi, S., Regoli, F., 2017. Plastics and microplastics in the oceans: From emerging pollutants to emerged threat. Mar. Environ. Res. https://doi.org/10.1016/j.marenvres.2016.05.012

Barrows, A.P.W., Cathey, S.E., Petersen, C.W., 2018. Marine environment microfiber

446 contamination: Global patterns and the diversity of microparticle origins. Environ. Pollut. 237,
447 275–284. https://doi.org/10.1016/j.envpol.2018.02.062

448 Bergmann, M., Mützel, S., Primpke, S., Tekman, M.B., Trachsel, J., Gerdts, G., 2019. White and
449 wonderful? Microplastics prevail in snow from the Alps to the Arctic. Sci. Adv. 5, eaax1157.
450 https://doi.org/10.1126/sciadv.aax1157

451 Bergmann, M., Wirzberger, V., Krumpen, T., Lorenz, C., Primpke, S., Tekman, M.B., Gerdts, G.,
452 2017. High Quantities of Microplastic in Arctic Deep-Sea Sediments from the
453 HAUSGARTEN Observatory. Environ. Sci. Technol. 51, 11000–11010.
454 https://doi.org/10.1021/acs.est.7b03331

455 Brahney, J., Hallerud, M., Heim, E., Hahnenberger, M., Sukumaran, S., 2020. Plastic rain in
456 protected areas of the United States. Science (80-.). 368, 1257–1260.
457 https://doi.org/10.1126/science.aaz5819

458 Choy, C.A., Robison, B.H., Gagne, T.O., Erwin, B., Firl, E., Halden, R.U., Hamilton, J.A., Katija,
459 K., Lisin, S.E., Rolsky, C., S. Van Houtan, K., 2019. The vertical distribution and biological
460 transport of marine microplastics across the epipelagic and mesopelagic water column. Sci.
461 Rep. 9, 7843. https://doi.org/10.1038/s41598-019-44117-2

462 Cincinelli, A., Scopetani, C., Chelazzi, D., Lombardini, E., Martellini, T., Katsoyiannis, A., Fossi,
463 M.C., Corsolini, S., 2017. Microplastic in the surface waters of the Ross Sea (Antarctica):
464 Occurrence, distribution and characterization by FTIR. Chemosphere 175, 391–400.
465 https://doi.org/10.1016/j.chemosphere.2017.02.024

466 Cole, M., Lindeque, P., Fileman, E., Halsband, C., Goodhead, R., Moger, J., Galloway, T.S., 2013.
467 Microplastic Ingestion by Zooplankton. Environ. Sci. Technol. 47, 6646–6655.
468 https://doi.org/10.1021/es400663f

469 Cózar, A., Martí, E., Duarte, C.M., García-de-Lomas, J., van Sebille, E., Ballatore, T.J., Eguíluz,
470 V.M., González-Gordillo, J.I., Pedrotti, M.L., Echevarría, F., Troublè, R., Irigoien, X., 2017.
471 The Arctic Ocean as a dead end for floating plastics in the North Atlantic branch of the
472 Thermohaline Circulation. Sci. Adv. 3, e1600582. https://doi.org/10.1126/sciadv.1600582

473 Davidson, K., Dudas, S.E., 2016. Microplastic Ingestion by Wild and Cultured Manila Clams
474 (Venerupis philippinarum) from Baynes Sound, British Columbia. Arch. Environ. Contam.
475 Toxicol. 71, 147–156. https://doi.org/10.1007/s00244-016-0286-4

476 Devriese, L.I., van der Meulen, M.D., Maes, T., Bekaert, K., Paul-Pont, I., Frère, L., Robbens, J.,
477 Vethaak, A.D., 2015. Microplastic contamination in brown shrimp (Crangon crangon,
478 Linnaeus 1758) from coastal waters of the Southern North Sea and Channel area. Mar. Pollut.
479 Bull. 98, 179–187. https://doi.org/10.1016/j.marpolbul.2015.06.051

480 Enders, K., Lenz, R., Stedmon, C.A., Nielsen, T.G., 2015. Abundance, size and polymer
481 composition of marine microplastics ≥10μm in the Atlantic Ocean and their modelled vertical
482 distribution. Mar. Pollut. Bull. 100, 70–81. https://doi.org/10.1016/j.marpolbul.2015.09.027

483 Gunnarsdóttir, R., Jenssen, P.D., Erland Jensen, P., Villumsen, A., Kallenborn, R., 2013. A review
484 of wastewater handling in the Arctic with special reference to pharmaceuticals and personal
485 care products (PPCPs) and microbial pollution. Ecol. Eng. 50, 76–85.
486 https://doi.org/10.1016/j.ecoleng.2012.04.025

487 Hansen, B., Bjornsen, P.K., Hansen, P.J., 1994. The size ratio between planktonic predators and
488 their prey. Limnol. Oceanogr. 39, 395–403. https://doi.org/10.4319/lo.1994.39.2.0395

489 Hoge, J., Leach, C., 2016. Epoxy resin infused boat hulls. Reinf. Plast. 60, 221–223.
490 https://doi.org/10.1016/j.repl.2016.01.002

491 Isobe, A., Uchida, K., Tokai, T., Iwasaki, S., 2015. East Asian seas: A hot spot of pelagic
492 microplastics. Mar. Pollut. Bull. 101, 618–623.
493 https://doi.org/10.1016/j.marpolbul.2015.10.042

494 Jacobsen, R.B., Hedeholm, R., Dominique, R., Wheeland, L., 2018. Sustainable Fisheries, in:
495 Adaptation Actions for A Changing Arctic - Perspectives from the Baffin Bay and Davis Strait
496 Region. Arctic Monitoring and Assessment Programme, Oslo, pp. 163–176.

497 Jambeck, J.R., Geyer, R., Wilcox, C., Siegler, T.R., Perryman, M., Andrady, A., Narayan, R., Law,
498 K.L., 2015. Plastic waste inputs from land into the ocean. Science (80-.). 347, 768–771.
499 https://doi.org/10.1126/science.1260352

500 Jespersen, A.M., Christoffersen, K., 1987. Measurements of chlorophyll—a from phytoplankton
501 using ethanol as extraction solvent. Arch. für Hydrobiol. 109, 445–454.

502 Jiang, Y., Yang, F., Zhao, Y., Wang, J., 2020. Greenland Sea Gyre increases microplastic pollution
503 in the surface waters of the Nordic Seas. Sci. Total Environ. 712, 136484.
504 https://doi.org/10.1016/j.scitotenv.2019.136484

505 Juul-Pedersen, T., Nielsen, T., Michel, C., Friis Møller, E., Tiselius, P., Thor, P., Olesen, M.,
506 Selander, E., Gooding, S., 2006. Sedimentation following the spring bloom in Disko Bay,
507 West Greenland, with special emphasis on the role of copepods. Mar. Ecol. Prog. Ser. 314,
508 239–255. https://doi.org/10.3354/meps314239

509 Kanhai, L.D.K., Gardfeldt, K., Krumpen, T., Thompson, R.C., O'Connor, I., 2020. Microplastics in
510 sea ice and seawater beneath ice floes from the Arctic Ocean. Sci. Rep. 10, 5004.
511 https://doi.org/10.1038/s41598-020-61948-6

512 Kanhai, L.D.K., Gårdfeldt, K., Lyashevska, O., Hassellöv, M., Thompson, R.C., O'Connor, I.,

513 2018. Microplastics in sub-surface waters of the Arctic Central Basin. Mar. Pollut. Bull. 130,
514 8–18. https://doi.org/10.1016/j.marpolbul.2018.03.011

515 Lebreton, L., Andrady, A., 2019. Future scenarios of global plastic waste generation and disposal.
516 Palgrave Commun. 5, 6. https://doi.org/10.1057/s41599-018-0212-7

517 Lebreton, L., Egger, M., Slat, B., 2019. A global mass budget for positively buoyant macroplastic
518 debris in the ocean. Sci. Rep. 9, 12922. https://doi.org/10.1038/s41598-019-49413-5

519 Levinsen, H., Nielsen, T.G., 2002. The trophic role of marine pelagic ciliates and heterotrophic
520 dinoflagellates in arctic and temperate coastal ecosystems: A cross-latitude comparison.
521 Limnol. Oceanogr. 47, 427–439. https://doi.org/10.4319/lo.2002.47.2.0427

522 Li, J., Green, C., Reynolds, A., Shi, H., Rotchell, J.M., 2018. Microplastics in mussels sampled
523 from coastal waters and supermarkets in the United Kingdom. Environ. Pollut. 241, 35–44.
524 https://doi.org/10.1016/j.envpol.2018.05.038

525 Liu, F., Olesen, K.B., Borregaard, A.R., Vollertsen, J., 2019. Microplastics in urban and highway
526 stormwater retention ponds. Sci. Total Environ. 671, 992–1000.
527 https://doi.org/10.1016/j.scitotenv.2019.03.416

528 Löder, M.G.J., Kuczera, M., Mintenig, S., Lorenz, C., Gerdts, G., 2015. Focal plane array detector-
529 based micro-Fourier-transform infrared imaging for the analysis of microplastics in
530 environmental samples. Environ. Chem. 12, 563. https://doi.org/10.1071/EN14205

531 Long, M., Moriceau, B., Gallinari, M., Lambert, C., Huvet, A., Raffray, J., Soudant, P., 2015.
532 Interactions between microplastics and phytoplankton aggregates: Impact on their respective
533 fates. Mar. Chem. 175, 39–46. https://doi.org/10.1016/j.marchem.2015.04.003

534 Lusher, A.L., Tirelli, V., O'Connor, I., Officer, R., 2015. Microplastics in Arctic polar waters: the

first reported values of particles in surface and sub-surface samples. Sci. Rep. 5, 14947. https://doi.org/10.1038/srep14947

Mai, L., Bao, L.-J., Shi, L., Wong, C.S., Zeng, E.Y., 2018. A review of methods for measuring microplastics in aquatic environments. Environ. Sci. Pollut. Res. 25, 11319–11332. https://doi.org/10.1007/s11356-018-1692-0

Mintenig, S.M., Int-Veen, I., Löder, M.G.J., Primpke, S., Gerdts, G., 2016. Identification of microplastic in effluents of waste water treatment plants using focal plane array-based micro-Fourier-transform infrared imaging. Water Res. https://doi.org/10.1016/j.watres.2016.11.015

Möhlenkamp, P., Purser, A., Thomsen, L., 2018. Plastic microbeads from cosmetic products: an experimental study of their hydrodynamic behaviour, vertical transport and resuspension in phytoplankton and sediment aggregates. Elem Sci Anth 6, 61. https://doi.org/10.1525/elementa.317

Morgana, S., Ghigliotti, L., Estévez-Calvar, N., Stifanese, R., Wieckzorek, A., Doyle, T., Christiansen, J.S., Faimali, M., Garaventa, F., 2018. Microplastics in the Arctic: A case study with sub-surface water and fish samples off Northeast Greenland. Environ. Pollut. 242, 1078–1086. https://doi.org/10.1016/j.envpol.2018.08.001

Mortensen, J., Bendtsen, J., Motyka, R.J., Lennert, K., Truffer, M., Fahnestock, M., Rysgaard, S., 2013. On the seasonal freshwater stratification in the proximity of fast-flowing tidewater outlet glaciers in a sub-Arctic sill fjord. J. Geophys. Res. Ocean. 118, 1382–1395. https://doi.org/10.1002/jgrc.20134

Mortensen, J., Lennert, K., Bendtsen, J., Rysgaard, S., 2011. Heat sources for glacial melt in a sub-Arctic fjord (Godthåbsfjord) in contact with the Greenland Ice Sheet. J. Geophys. Res. 116, C01013. https://doi.org/10.1029/2010JC006528

558 Mu, J., Zhang, S., Qu, L., Jin, F., Fang, C., Ma, X., Zhang, W., Wang, J., 2019. Microplastics
559 abundance and characteristics in surface waters from the Northwest Pacific, the Bering Sea,
560 and the Chukchi Sea. Mar. Pollut. Bull. 143, 58–65.
561 https://doi.org/10.1016/j.marpolbul.2019.04.023

562 Napper, I.E., Thompson, R.C., 2016. Release of synthetic microplastic plastic fibres from domestic
563 washing machines: Effects of fabric type and washing conditions. Mar. Pollut. Bull. 112, 39–
564 45. https://doi.org/10.1016/j.marpolbul.2016.09.025

565 Obbard, R.W., 2018. Microplastics in Polar Regions: The role of long range transport. Curr. Opin.
566 Environ. Sci. Heal. 1, 24–29. https://doi.org/10.1016/j.coesh.2017.10.004

567 Obbard, R.W., Sadri, S., Wong, Y.Q., Khitun, A. a., Baker, I., Thompson, R.C., 2014. Global
568 warming releases microplastic legacy frozen in Arctic Sea ice. Earth's Futur. 2, 315–320.
569 https://doi.org/10.1002/2014EF000240

570 PAME, 2019. Desktop Study on Marine Litter including Microplastics in the Arctic.

571 Peeken, I., Primpke, S., Beyer, B., Gütermann, J., Katlein, C., Krumpen, T., Bergmann, M.,
572 Hehemann, L., Gerdts, G., 2018. Arctic sea ice is an important temporal sink and means of
573 transport for microplastic. Nat. Commun. 9, 1505. https://doi.org/10.1038/s41467-018-03825-
574 5

575 Peng, X., Chen, M., Chen, S., Dasgupta, S., Xu, H., Ta, K., Du, M., Li, J., Guo, Z., Bai, S., 2018.
576 Microplastics contaminate the deepest part of the world's ocean. Geochemical Perspect. Lett.
577 9, 1–5. https://doi.org/10.7185/geochemlet.1829

578 Pirc, U., Vidmar, M., Mozer, A., Kržan, A., 2016. Emissions of microplastic fibers from microfiber
579 fleece during domestic washing. Environ. Sci. Pollut. Res. https://doi.org/10.1007/s11356-016-

580 7703-0

581 PlasticsEurope, 2019. Plastics - the Facts 2019.

582 Porter, A., Lyons, B.P., Galloway, T.S., Lewis, C., 2018. Role of Marine Snows in Microplastic
583 Fate and Bioavailability. Environ. Sci. Technol. 52, 7111–7119.
584 https://doi.org/10.1021/acs.est.8b01000

585 Primpke, S., Cross, R.K., Mintenig, S.M., Simon, M., Vianello, A., Gerdts, G., Vollertsen, J., 2020.
586 EXPRESS: Toward the Systematic Identification of Microplastics in the Environment:
587 Evaluation of a New Independent Software Tool (siMPle) for Spectroscopic Analysis. Appl.
588 Spectrosc. https://doi.org/10.1177/0003702820917760

589 Primpke, S., Lorenz, C., Rascher-Friesenhausen, R., Gerdts, G., 2016. Analytical Methods An
590 automated approach for microplastics analysis using focal plane array (FPA) FTIR microscopy
591 and image analysis. J. Name 8, 1–224. https://doi.org/10.1039/x0xx00000x

592 Setälä, O., Fleming-Lehtinen, V., Lehtiniemi, M., 2014. Ingestion and transfer of microplastics in
593 the planktonic food web. Environ. Pollut. 185, 77–83.
594 https://doi.org/10.1016/j.envpol.2013.10.013

595 Simon, M., van Alst, N., Vollertsen, J., 2018. Quantification of microplastic mass and removal rates
596 at wastewater treatment plants applying Focal Plane Array (FPA)-based Fourier Transform
597 Infrared (FT-IR) imaging. Water Res. 142, 1–9. https://doi.org/10.1016/j.watres.2018.05.019

598 Sun, X., Li, Q., Zhu, M., Liang, J., Zheng, S., Zhao, Y., 2017. Ingestion of microplastics by natural
599 zooplankton groups in the northern South China Sea. Mar. Pollut. Bull. 115, 217–224.
600 https://doi.org/10.1016/j.marpolbul.2016.12.004

601 Tamminga, M., Hengstmann, E., Fischer, E.K., 2018. Microplastic analysis in the South Funen

602 Archipelago, Baltic Sea, implementing manta trawling and bulk sampling. Mar. Pollut. Bull.
603 128, 601–608. https://doi.org/10.1016/j.marpolbul.2018.01.066

604 Tekman, M.B., Wekerle, C., Lorenz, C., Primpke, S., Hasemann, C., Gerdts, G., Bergmann, M.,
605 2020. Tying up loose ends of microplastic pollution in the Arctic: Distribution from the sea
606 surface, through the water column to deep-sea sediments at the HAUSGARTEN observatory.
607 Environ. Sci. Technol. acs.est.9b06981. https://doi.org/10.1021/acs.est.9b06981

608 van Sebille, E., England, M.H., Froyland, G., 2012. Origin, dynamics and evolution of ocean
609 garbage patches from observed surface drifters. Environ. Res. Lett. 7, 044040.
610 https://doi.org/10.1088/1748-9326/7/4/044040

611 van Sebille, E., Wilcox, C., Lebreton, L., Maximenko, N., Hardesty, B.D., van Franeker, J.A.,
612 Eriksen, M., Siegel, D., Galgani, F., Law, K.L., 2015. A global inventory of small floating
613 plastic debris. Environ. Res. Lett. 10, 124006. https://doi.org/10.1088/1748-
614 9326/10/12/124006

615 Vianello, A., Jensen, R.L., Liu, L., Vollertsen, J., 2019. Simulating human exposure to indoor
616 airborne microplastics using a Breathing Thermal Manikin. Sci. Rep. 9, 8670.
617 https://doi.org/10.1038/s41598-019-45054-w

618 von Friesen, L.W., Granberg, M.E., Pavlova, O., Magnusson, K., Hassellöv, M., Gabrielsen, G.W.,
619 2020. Summer sea ice melt and wastewater are important local sources of microlitter to
620 Svalbard waters. Environ. Int. 139, 105511. https://doi.org/10.1016/j.envint.2020.105511

621 Vroom, R.J.E., Koelmans, A.A., Besseling, E., Halsband, C., 2017. Aging of microplastics
622 promotes their ingestion by marine zooplankton. Environ. Pollut. 231, 987–996.
623 https://doi.org/10.1016/j.envpol.2017.08.088

624 Welden, N.A., Abylkhani, B., Howarth, L.M., 2018. The effects of trophic transfer and
625 environmental factors on microplastic uptake by plaice, Pleuronectes plastessa, and spider
626 crab, Maja squinado. Environ. Pollut. 239, 351–358.
627 https://doi.org/10.1016/j.envpol.2018.03.110

628 Woodall, L.C., Sanchez-Vidal, A., Canals, M., Paterson, G.L.J., Coppock, R., Sleight, V., Calafat,
629 A., Rogers, A.D., Narayanaswamy, B.E., Thompson, R.C., 2014. The deep sea is a major sink
630 for microplastic debris. R. Soc. Open Sci. 1, 140317–140317.
631 https://doi.org/10.1098/rsos.140317

632

633 **Graphical abstract**

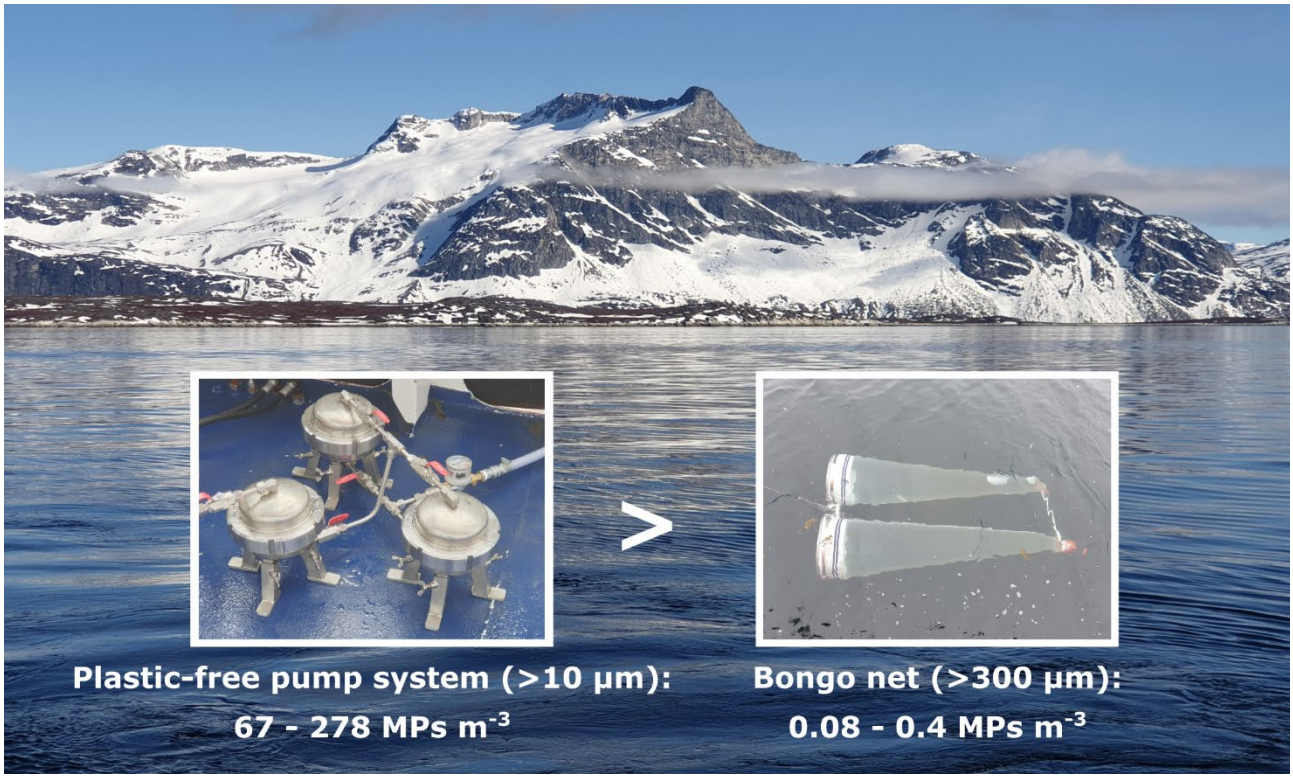

634